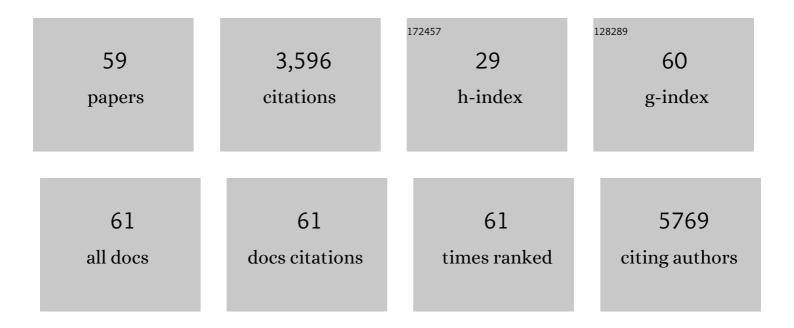
Cheol-Hee Ahn

List of Publications by Year in descending order

Source: https://exaly.com/author-pdf/11122721/publications.pdf Version: 2024-02-01



#	Article	IF	CITATIONS
1	Recent Trend of Ultrasound-Mediated Nanoparticle Delivery for Brain Imaging and Treatment. ACS Applied Materials & Interfaces, 2023, 15, 120-137.	8.0	10
2	Ultrasound-triggered imaging and drug delivery using microbubble-self-aggregate complexes. Journal of Biomaterials Science, Polymer Edition, 2022, 33, 57-76.	3.5	3
3	Biodegradable poly(lactide-co-glycolide) microspheres encapsulating hydrophobic contrast agents for transarterial chemoembolization. Journal of Biomaterials Science, Polymer Edition, 2022, 33, 409-425.	3.5	4
4	Advances in Ion Conducting Membranes and Binders for High Temperature Polymer Electrolyte Membrane Fuel Cells. Polymer Reviews, 2022, 62, 789-825.	10.9	12
5	Novel Potentially Biobased Copolyesters Comprising 1,3-Butanediol, 1,4-Cyclohexanedimethanol and Dimethyl Terephthalate; Effect of Different Catalysts on Polymerization Behavior. Macromolecular Research, 2022, 30, 51-60.	2.4	3
6	Emerging Albumin-Binding Anticancer Drugs for Tumor-Targeted Drug Delivery: Current Understandings and Clinical Translation. Pharmaceutics, 2022, 14, 728.	4.5	33
7	Cathepsin B-Overexpressed Tumor Cell Activatable Albumin-Binding Doxorubicin Prodrug for Cancer-Targeted Therapy. Pharmaceutics, 2022, 14, 83.	4.5	15
8	Dispersing Agents Impact Performance of Protonated Phosphonic Acid High-Temperature Polymer Electrolyte Membrane Fuel Cells. ACS Energy Letters, 2022, 7, 1642-1647.	17.4	11
9	How Did Conventional Nanoparticle-Mediated Photothermal Therapy Become "Hot―in Combination with Cancer Immunotherapy?. Cancers, 2022, 14, 2044.	3.7	15
10	Theragnostic Glycol Chitosan-Conjugated Gold Nanoparticles for Photoacoustic Imaging of Regional Lymph Nodes and Delivering Tumor Antigen to Lymph Nodes. Nanomaterials, 2021, 11, 1700.	4.1	15
11	A supramolecular host-guest interaction-mediated injectable hydrogel system with enhanced stability and sustained protein release. Acta Biomaterialia, 2021, 131, 286-301.	8.3	29
12	Thiol-Responsive Gold Nanodot Swarm with Glycol Chitosan for Photothermal Cancer Therapy. Molecules, 2021, 26, 5980.	3.8	4
13	Surface Modification of Polystyrene Beads with Sulfonamide Derivatives and Application to Water Softening System. Macromolecular Research, 2020, 28, 172-178.	2.4	3
14	Self-Healable Dielectric Polydimethylsiloxane Composite Based on Zinc-Imidazole Coordination Bond. Macromolecular Research, 2019, 27, 435-443.	2.4	18
15	Activatable NIRF/MRI dual imaging probe using bio-inspired coating of glycol chitosan on superparamagnetic iron oxide nanoparticles. Journal of Industrial and Engineering Chemistry, 2019, 76, 403-409.	5.8	9
16	Photoacoustic imaging of cancer cells with glycol-chitosan-coated gold nanoparticles as contrast agents. Journal of Biomedical Optics, 2019, 24, 1.	2.6	32
17	High-Performance Printed Circuit Board Materials Based on Benzoxazine and Epoxy Blend System. Macromolecular Research, 2018, 26, 388-393.	2.4	25
18	Tissue adhesive FK506–loaded polymeric nanoparticles for multi–layered nano–shielding of pancreatic islets to enhance xenograft survival in a diabetic mouse model. Biomaterials, 2018, 154, 182-196.	11.4	43

CHEOL-HEE AHN

#	Article	IF	CITATIONS
19	Thrombin-activatable fluorescent peptide incorporated gold nanoparticles for dual optical/computed tomography thrombus imaging. Biomaterials, 2018, 150, 125-136.	11.4	79
20	Xenotransplantation of layer-by-layer encapsulated non-human primate islets with a specified immunosuppressive drug protocol. Journal of Controlled Release, 2017, 258, 10-21.	9.9	33
21	Quantitative Imaging of Cerebral Thromboemboli In Vivo. Stroke, 2017, 48, 1376-1385.	2.0	15
22	Single synchronous delivery of FK506-loaded polymeric microspheres with pancreatic islets for the successful treatment of streptozocin-induced diabetes in mice. Drug Delivery, 2017, 24, 1350-1359.	5.7	29
23	Nano-sized metabolic precursors for heterogeneous tumor-targeting strategy using bioorthogonal click chemistry inÂvivo. Biomaterials, 2017, 148, 1-15.	11.4	51
24	Combined Near-infrared Fluorescent Imaging and Micro-computed Tomography for Directly Visualizing Cerebral Thromboemboli. Journal of Visualized Experiments, 2016, , .	0.3	4
25	Study on chemotaxis and chemokinesis of bone marrow-derived mesenchymal stem cells in hydrogel-based 3D microfluidic devices. Biomaterials Research, 2016, 20, 25.	6.9	24
26	Direct Imaging of Cerebral Thromboemboli Using Computed Tomography and Fibrin-targeted Gold Nanoparticles. Theranostics, 2015, 5, 1098-1114.	10.0	101
27	Biocompatible Glycol Chitosan-Coated Gold Nanoparticles for Tumor-Targeting CT Imaging. Pharmaceutical Research, 2014, 31, 1418-1425.	3.5	108
28	Hypoxia-responsive polymeric nanoparticles for tumor-targeted drug delivery. Biomaterials, 2014, 35, 1735-1743.	11.4	296
29	Targeted multimodal imaging modalities. Advanced Drug Delivery Reviews, 2014, 76, 60-78.	13.7	113
30	Fluorescent Dye Labeled Iron Oxide/Silica Core/Shell Nanoparticle as a Multimodal Imaging Probe. Pharmaceutical Research, 2014, 31, 3371-3378.	3.5	32
31	Effect of molecular architecture on micellization, drug loading and releasing of multi-armed poly(ethylene glycol)-b-poly(ε-caprolactone) star polymers. Colloid and Polymer Science, 2013, 291, 1817-1827.	2.1	21
32	Hyperacute direct thrombus imaging using computed tomography and gold nanoparticles. Annals of Neurology, 2013, 73, 617-625.	5.3	39
33	Development of a pH sensitive nanocarrier using calcium phosphate coated gold nanoparticles as a platform for a potential theranostic material. Macromolecular Research, 2012, 20, 319-326.	2.4	24
34	Tumorâ€Targeting Gold Particles for Dual Computed Tomography/Optical Cancer Imaging. Angewandte Chemie - International Edition, 2011, 50, 9348-9351.	13.8	116
35	Conjugation of histidine derivatives to PEGylated poly(L-lysine-co-L-phenylalanine) copolymer as a non-viral gene carrier. Macromolecular Research, 2010, 18, 545-550.	2.4	6
36	pH dependent drug release system using micelles stabilized by cationic drugs. Macromolecular Research, 2010, 18, 686-689.	2.4	6

CHEOL-HEE AHN

#	Article	IF	CITATIONS
37	Blends of Oppositely Charged PEG–PPG–PEG Copolymers Displaying Improved Physical Thermogelling Properties. Macromolecular Chemistry and Physics, 2010, 211, 692-697.	2.2	9
38	Reduction‧ensitive Selfâ€Aggregates as a Novel Delivery System. Macromolecular Chemistry and Physics, 2010, 211, 956-961.	2.2	20
39	Thermo-sensitive, injectable, and tissue adhesive sol–gel transition hyaluronic acid/pluronic composite hydrogels prepared from bio-inspired catechol-thiol reaction. Soft Matter, 2010, 6, 977.	2.7	336
40	"One-Step―Detection of Matrix Metalloproteinase Activity Using a Fluorogenic Peptide Probe-Immobilized Diagnostic Kit. Bioconjugate Chemistry, 2010, 21, 1378-1384.	3.6	21
41	Matrix Metalloproteinase Sensitive Gold Nanorod for Simultaneous Bioimaging and Photothermal Therapy of Cancer. Bioconjugate Chemistry, 2010, 21, 2173-2177.	3.6	92
42	Heparinâ€Coated Gold Nanoparticles for Liverâ€Specific CT Imaging. Chemistry - A European Journal, 2009, 15, 13341-13347.	3.3	146
43	Micelle Behavior of Copolymers Composed of Linear and Hyperbranched Blocks in Aqueous Solution. Macromolecular Chemistry and Physics, 2009, 210, 1734-1738.	2.2	11
44	A novel pH-sensitive PEG-PPG-PEG copolymer displaying a closed-loop sol–gel–sol transition. Journal of Materials Chemistry, 2009, 19, 8198.	6.7	27
45	Polymeric Nanoparticle-Based Activatable Near-Infrared Nanosensor for Protease Determination In Vivo. Nano Letters, 2009, 9, 4412-4416.	9.1	149
46	Dye-Condensed Biopolymeric Hybrids: Chromophoric Aggregation and Self-Assembly toward Fluorescent Bionanoparticles for Near Infrared Bioimaging. Chemistry of Materials, 2009, 21, 5819-5825.	6.7	90
47	A Nearâ€Infraredâ€Fluorescenceâ€Quenched Goldâ€Nanoparticle Imaging Probe for Inâ€Vivo Drug Screening a Protease Activity Determination. Angewandte Chemie - International Edition, 2008, 47, 2804-2807.	nd 13.8	310
48	Temperature/pH-Sensitive Hydrogels Prepared from Pluronic Copolymers End-Capped with Carboxylic Acid Groups via an Oligolactide Spacer. Macromolecular Rapid Communications, 2007, 28, 1172-1176.	3.9	73
49	Synthesis and characterization of Poly(L-lysine-co-L-proline) as a non-viral gene delivery vector. Macromolecular Research, 2006, 14, 129-131.	2.4	5
50	Preparation and characterization of cisplatin-incorporated chitosan hydrogels, microparticles, and nanoparticles. Macromolecular Research, 2006, 14, 573-578.	2.4	34
51	Synthesis of Novel Biodegradable Cationic Dendrimers. Macromolecular Rapid Communications, 2006, 27, 1608-1614.	3.9	14
52	Drug release behavior of poly(ε-caprolactone)-b-Poly(acrylic acid) Shell Crosslinked Micelles below the Critical Micelle Concentration. Macromolecular Research, 2005, 13, 397-402.	2.4	31
53	Design and Synthesis of a New pH Sensitive Polymeric Sensor Using Fluorescence Resonance Energy Transfer. Chemistry of Materials, 2005, 17, 6213-6215.	6.7	45
54	Synthesis of biodegradable multi-block copolymers of poly(l-lysine) and poly(ethylene glycol) as a non-viral gene carrier. Journal of Controlled Release, 2004, 97, 567-574.	9.9	38

CHEOL-HEE AHN

#	Article	IF	CITATIONS
55	Synthesis and Micellization of Star-Shaped Poly(ethylene glycol)-block-Poly(É>-caprolactone). Macromolecular Chemistry and Physics, 2004, 205, 1684-1692.	2.2	70
56	Biodegradable Poly(ethylene glycol)-co-poly(l-lysine)-g-histidine Multiblock Copolymers for Nonviral Gene Delivery. Macromolecules, 2004, 37, 1903-1916.	4.8	115
57	Biodegradable poly(ethylenimine) for plasmid DNA delivery. Journal of Controlled Release, 2002, 80, 273-282.	9.9	292
58	Epitaxial Adsorption of Monodendron-Jacketed Linear Polymers on Highly Oriented Pyrolytic Graphite. Langmuir, 2000, 16, 6862-6867.	3.5	70
59	Molecular imaging of monodendron jacketed linear polymers by scanning force microscopy. Macromolecular Rapid Communications, 1998, 19, 359-366.	3.9	126